

Brake Pad Performance Characteristic Assessment Methods

Gülşah Akıncıoğlu^{1*}, Sıtkı Akıncıoğlu¹, Hasan Öktem², İlyas Uygur³

0000-0002-4768-4935, 0000-0003-4073-4837, 0000-0003-2526-8364, 0000-0002-8744-5082

¹ Machine Design and Construction, Gumusova Vocational School, Duzce University, Duzce, 81850, Turkey

² Department of Machine and Metal Technologies, Hereke Asım Kocabıyık Vocational School, Kocaeli University, Turkey

³ Department of Mechanical Engineering, Engineering Faculty, Duzce University, Duzce, 81100, Turkey

Abstract

Along with the developing technology, expectations for improved automobile brake pads are also rising. Research on higher performance brake pads is continuing at a rapid pace. It is also recognized that in this field, widespread efforts are being made towards the production of brake pads which are economical, environmentally friendly and do not pose risks to human health. In recent years, non-industrial waste products have also been used as additives in brake pads, thus contributing to local economy. Performance tests have to be carried out so that the brake pads produced with the new compositions can be used. For this reason, the performance tests of the brake pads are important. This study brings a new overview via an investigation of the methods applied in determining their performance characteristics.

Keywords: Brake pads, Review, Testing method, Performance characteristic, Test devices.

Review Article

<https://doi.org/10.30939/ijastech..848266>

Received 28.12.2020

Revised 06.02.2021

Accepted 10.02.2021

* Corresponding author

Gülşah Akıncıoğlu

gulsahakincioglu@duzce.edu.tr

Address: Machine Design and Construction, Gumusova Vocational School, Duzce University, Duzce, 81850, Turkey

Phone:+903122028653

1. Introduction

In every vehicle, the brake pads play an important role in the braking system [1, 2]. The first brakes consisted of a rope wound around the back axle of a horse carriage, or a piece of wood pressed against the rim of the wheel. Modern brake pad materials share many similarities with these primitive brakes [3]. Along with the development of automotive technology, many studies have been carried out in the search for cheap, high-performance, environmentally friendly and safe brake pads. The brake pad lining generates friction against the rotating disc to perform the task of braking [4]. During the process of breaking the moving vehicle, this friction converts the kinetic energy to thermal energy. Thus, the material used for brake friction is a crucial element in the process [5]. It is important to examine the testing procedures applied to the brake pads produced using different additive materials [6]. If test results of newly created compositions are within acceptable standards, the new brake pads can be commercialized. These tests include those for hardness, density, shear, compressibility, water-oil absorption and friction-wear [7]. Friction-wear tests can be performed using many

differently designed devices (pin-on-disc testers, Krauss machines, scratch testing instruments, brake inertia dynamometers, etc.) [8-12]. WanNik et al. [13] investigated the friction performance of 0.6%, 1%, 1.5% and 2% boron-augmented brake pads. The researchers prepared samples of brake pads for measurement of friction coefficients, hardness, thickness loss, surface roughness, porosity and specific gravity. They used a commercial ZMF brake pad for comparison. Results of the bootstrap analyses showed a great difference between the boron-supplemented and the commercial brake pads in the coefficient of friction, hardness and brake fines. Qi et al. [14] examined the friction and wear behaviors of environmentally friendly brake pads made by using walnut shell powder (WSP). The experimental results indicated that the number of WSP-added friction coats contributed positively to the stability and wear resistance. Singaravelu et al. [15] They investigated the effects of the powder obtained by chemical and thermal processing of crab shell powder on the performance of brake pads. Thermal stability was found using thermogravimetric analysis of brake pads. They performed performance tests of brake pads with the Chase tester. Test results show that thermally treated crab shell powder-based

brake pads show better thermal stability thanks to a 37% coal residue. Chemical treated crab shell powder-based brake pads had better fade and recovery properties with a 1.71% fading rate and 99.86% recovery rate due to better heat dissipation and coarse texture. Manoharan et al. [16] investigated the effect of red mud as an abrasive on brake pads and iron sulfide as a lubricant. They used a Chase-type tester for the tribological performance of two different brake pads. As a result of the tests, they found that the synergistic effect of red sludge and iron sulfur particles in friction composites showed stable fading and recovery behaviors. It can be concluded that iron sulfide-based friction composites show less wear rate. In their experimental study, Nagesh et al. [17] compared brake pad constituents used at different ratios with a previously made composition in terms of their effects on the physical and tribological properties of the starting material. The obtained results displayed similar values. Bahari et al. investigated the hardness and resistance of automobile brake pads with 10% and 30% additions of rice husk dust (RHD). They reported that the RHD, especially at 30%, had a good effect on the hardness properties of the new pads [18]. Polymer composites have a wide range of applications as brake friction materials. Fan et al. examined the wear resistance of brake pads made using C/SiC. In this study, the main wear observed included grain, oxidation, fatigue and adhesion wear. They believed that the hard SiC grains were the cause of the grain wear [19]. Kukutschova et al. investigated the wear performance and wear abrasion of semi-metallic brake pads. Randomly selected pads milled for 10 min were compared to pads after braking and tested on a dynamometer. As a result, they observed that the wear particles after braking were in a different form than those of the milled pads [20]. Kim et al. [11] used four abrasive materials (zircon, magnesia, quartz, and SiC) in their study of brake pad vibration and wear behavior. The results ranked the coefficient of friction in the order of SiC > zircon > quartz > magnesia. Stadler et al. [21] evaluated the friction behavior of C/C-SiC brake discs with sintered brake pads. The wear was mostly in the graphite and SiC bearing discs, causing the graphite material to soften. The chemical composition and structure and of the friction surface differed from that of the mass. There are many studies on brake linings. Many of these have focused on reducing brake costs, improving performance, or using alternative dusts by obtaining new composites [22]. Many tests are applied to brake pads produced with new compositions [23]. In the studies conducted, performance tests were applied in many different ways. It may be useful to compare the test methods that have been applied to brake pads.

An examination of these studies showed that brake pads of many different components have been produced and tested. The reasons for producing brake pads from different components can include efforts to reduce the product cost, to increase the braking efficiency, to avoid hazards to the environment and health, and to contribute to the local economy by increasing the industrial value of local materials. This study aimed to survey and evaluate the methods used to test brake pads.

2. Brake Pad Testing Methods

2.1 Hardness test

High hardness is attributable to the increase in bonding. Softer material results in a larger contact area, and thus, a higher coefficient of friction is achieved [21]. Increasing the hardness of the brake pad causes an increase in the wear resistance [24]. Therefore, in order to determine their hardness, it is vital that tests be performed on brake pads formulated with different compositions. Many different systems (Brinell, Rockwell-R, Rockwell-S, Rockwell-B, Shore D, Vikers and Mohs hardness scales) are used to measure the hardness of brake pads. Hardness tests are done according to ASTM D256 and ASTM D785 standards. The hardness values of brake pads are influenced by their compositions and production methods [25] The sieve grade is decreased according to the hardness values of the brake pads [26], whereas the hardness of the brake pads increases with the increasing weight percentage of the resin [27]. Moreover, the the hardness of the metallic matrix can be increased by addition of SiC [21]. Manoharan et al. [28] were chosen as the friction modifier in the brake pad, three forms of graphite particles: thermally pure vein graphite (VG), thermally pure flake graphite (FG) and refined expandable graphite (EG). Since the interlayer distances measured from X-ray diffraction plots are high, the stiffness for EGC is low compared to VGC and FGC due to poor interlayer bonding of EG particles.

2.2 Density test

In addition to the frictional properties, product density is an important parameter in brake pads [29]. Depending on the composition used, the dimensions of the dust, the method of molding, and the heat treatment applied, the density of brake pads may vary [30]. The properties and proportions of the materials used as additives affect the density of brake pads. Manoharan et al. [28] they used thermally pure core graphite (VG), thermally pure flake graphite (FG) and refined expandable graphite (EG) in the brake pad. They found that the lining using pure vein graphite (VG) exhibited higher density due to the presence of impurities in the particles. The VG particle is very small in size and very close to each other due to gravitational forces. This finer particle size fills the composite area of the brake pad, increasing the packaging capability, they noted, resulting in higher density. However, FG has lower density which may be due to better compacted porosity behavior. The density difference of graphite particles is mainly due to the geological phenomenon acting on carbon deposits in the metamorphic or magmatic state, which can have biologically different origins. Ideally, they concluded that higher density contributes to higher stiffness. Density tests were conducted on brake pad samples using Archimedes' principle according to ASTM D792 [24, 27, 31]. Densities were measured and theoretically calculated by immersing the pad (cut in such a way as to fit the density kit) in pure water. Equation (1) expresses the formula for density calculation.

$$\text{Density (g/cm}^3\text{)} = \frac{\text{Dry Weight (g)}}{\text{Dry weight (g)} - \text{Wet weight (g)}} \quad (1)$$

2.3 Porosity, water and oil absorption tests

The friction should be maintained at a moderate level of stability covering a wide variety of environments, temperatures, loads, and speeds [4]. The amount of water absorbed can be measured by submerging brake pads in oil and water. The water and oil absorption test are conducted according to SEA 20/50 and ASTM D570-98 standards for the purpose of evaluating the porosity of the brake pads depending on the amount of oil and water they absorb. Porosity enables absorption of heat and energy, which for the brake pad system is a very important function. Porosity is necessary for the understanding of the form and construction of the various materials used. Low porosity results in high friction coefficients and wear rates. Some porosity is necessary for brake pads in order to reduce the effects on the friction coefficient caused by water and oil. Porosity tests are carried out in accordance with JIS D 4418-1996 standards [25]. After keeping brake pads in oil for 24 h, Öktem et al. measured their weight, stiffness and size. They found that in the oil-soaked brake pads, the hardness had decreased, while the size had increased only at the micron level [32]. Friction-induced film formation can be affected by water. It then follows that the braking behavior stability can be affected by this film formation [33]. The density of EG is lower compared to VG and FG, as the researchers [28] fill the cavity with the coarse particle size of

EG particles leaving sufficient porosity. The formula for calculating water and oil absorption is given as Equation (2).

$$\text{Water and oil absorption (\%)} = \left(\frac{B-A}{A \times 100} \right) \quad (2)$$

Here, A is the initial weight and B is the final weight.

2.4 Shear test

The shear test is conducted by separating the pad from the sheet by applying an axial and radial force and measuring the amount of the brake pad remaining on the disc sheet. The applied axial force must be in a range between 3 and 5 N/mm². The radial force is perpendicular to the surface of the brake pad and the axial force. Shear tests are carried out according to ISO 6312, SEA J840B and JIS 4422: 1995 standards (Table 1). As a result of this test, a minimum of 80% of the sheet surfaces must remain on the pad. Saikrishnan et al. [34] investigated the effect on the tribological performance of brake pads compared to commercially available iron-aluminum copper alloy, iron and aluminum powders. Their main purpose is to replace copper from frictional composite formulations. Cold shear strength of brake pads measured at room temperature according to ISO-6312. In this test, the improved brake pad with backplate was placed in the shear test rig. A side load is applied to the surface of the brake pad while applying another load in the vertical direction using a mallet. The load was applied gradually until it failed. It was found that the shear strength gives an overview of the strength between the backplate and the friction material.

Table 1. Brake pad shear test standards

| | ISO 6312:2001 | JIS 4422:1995 | SAE J840B:1998 |
|-----------------------------|------------------|------------------|-------------------|
| Ram offset | 1.0 mm | 1.0 mm | 0.25-0.51 mm |
| Constant speed rate applied | 10 mm/min | 10 mm/min | 10 mm/min |
| Constant load rate applied | 4500 N/s | 4500 N/s | - |
| Hot test | 300 °C | - | 205 °C |

2.5 Microstructural analyses

Microstructural analyses are conducted to evaluate the dust distribution in the brake pad composition and to examine the erosion on the brake pad surface. This essential analysis is used to determine the brake pad characteristics, the compatibility of the constituents, and their homogeneous distribution within new compositions.

2.5.1 SEM (scanning electron microscopy) analysis

The samples must be prepared carefully so that SEM images can be taken. The conductivity of the surface of the brake pad must be high enough to obtain SEM images. Particularly in the case of naturally-doped brake pads with low electrical conductivity, coatings are required in order to increase the conductivity and attain better microstructural images, so samples are coated with gold before the SEM imaging to improve the results. A number of studies have used the back-scattered electron (BSE)

mode for brake pad imaging [14, 35]. In normal mode, the elements of the microstructures are unclear. The BSE mode, being more sensitive and having greater resolution, easily distinguishes each element that forms the original. In many studies, analysis via SEM has been used to investigate different features of the produced brake pads, e.g., that of Singh and Patnaik. They examined pads augmented with lapinus and aramid and observed adhesive wear in the SEM images that was caused by the lapinus fiber [36]. Yun et al. [37] found that the environmental wear brake pads have less surface wear. Mohanty and Chug [38] utilized the SEM images of micron-sized fly ash dust additions in sample brake pads and examined the friction surface formation and characteristics. The plastic deformation of the soft aluminum fibers was revealed. The fibers in the composites had been contaminated when excessive contact took place. Xin et al. [39] evaluated SEM images of the sisal particles and friction surface in pad samples produced with sisal fibers. At 150 °C, the

main wear behavior on the fibers consisted of cutting abrasion, and on the matrix of fatigue cracking. Decomposition of the sisal fibers began when surface temperatures rose above 250 °C. Qi et al. [14] found irregularly formed friction surfaces in the SEM images of brake pads produced using walnut shell. Fu et al. [40] evaluated the flax fibers, basalt fibers and the friction surfaces in SEM images of brake pads reinforced with flax fibers. Moreover, Fan et al. [41] found that the most abrasion was observed in the SEM images of the sample with the highest Al₂O₃ content. According to the SEM images, with the increase in temperature, the stibnite patch population on the friction surface increased and individual steel fibers were deformed and spread. Vijay et al. [42] have developed copper-free brake pads using molybdenum disulfide with coarse, fine and super fine particle size. Tribological tests were conducted using the Chase test according to IS2742 standards. The results showed that coarse size molybdenum disulfide-based brake pads had better thermal stability with good fading and recovery properties leading to less wear than the other two composites. Scanning electron microscopy and energy dispersion analysis helped investigate the wear behavior of brake friction composite samples tested by Chase. Singaravelu et al. [43] discussed the development of five different brake friction composites according to the standard of Indian scenario brake pads by replacing different cashew friction powders. They used Scanning Electron Microscopy combined with elemental mapping to illuminate the retransfer and surface properties of the dynamically tested brake pads. The results demonstrated good fading, wear resistance and recovery properties of the boron-graphite modified friction powder-based brake pads due to their thermally stable and heat dissipation properties. Wear of composites is a complex phenomenon with multiple thermally activated mechanisms. The increase in friction increases the third body unevenness during braking. Although it increases friction, it is a part that breaks from the friction material at a microscopic level. This causes plowing on the mating surface causing rotor wear. This plow again produces iron oxide due to tribo-oxidation at the mating surface, which increases abrasive wear. The presence of iron oxide is confirmed by basic mapping in the following sections.

2.5.2 EDAX (Energy-dispersive X-ray) analysis

Energy-dispersive X-ray (EDAX) images are used to determine the quantities and elements contained in composites. The EDAX analyses on the SEM images of the samples enable determination of the elements forming the composition. The distribution of the specified elements in the microstructure can also be identified. Thus, the interaction of the dusts forming the brake pads and their mechanical properties can be evaluated. Qi et al. studied EDAX images of walnut shell powder-coated pads which indicated that the amount of carbon and iron had decreased with the increase of the amount of walnut shell [14]. Fu et al. [40] found dust materials such as vermiculite, zircon, natural graphite and barite in EDAX images of pads using flax fiber. Eriksson and Jacobson [44] examined the EDAX images of the

brake pads for the Volvo 850 automobile. In these images, they observed the main items that constituted the brake pads. They also detected iron and oxygen. Kim et al. [11] used abrasive SiC, zircon, quartz and magnesia powders in brake pad samples and detected these abrasives on the surfaces of the pads in EDAX analyses. The surface analyses of brake pad samples made by Dadkar et al. are shown in Fig. 1.

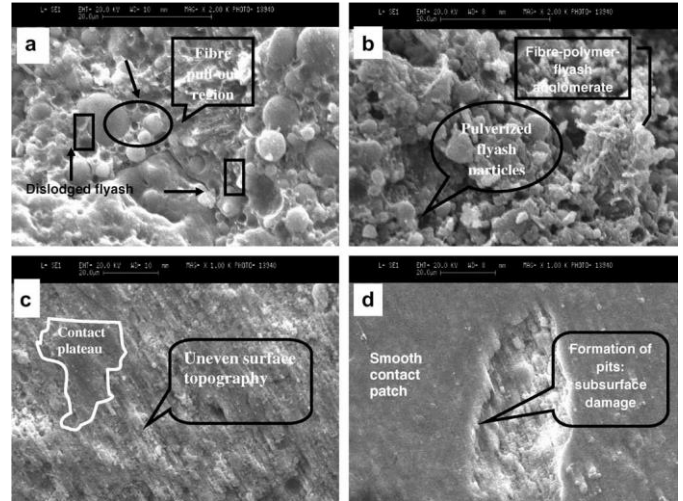


Fig. 1. EDAX micrographs of samples: (a) and (b) at low magnification; (c) and (d) at high magnification [45]

The morphology of the surface wear revealed many well-dispersed groove marks and several random areas of compacted wear debris, which made the friction surface appear smooth and unbroken [45].

2.6 Friction and wear tests

The safety and braking performance can be directly affected by the material wear rate [46], which makes wear tests among the most important tests used to determine brake pad performance. Tribological systems are the technical systems that occur with wear and friction [47]. Braking (in vehicles) is a tribological occurrence, thus confirming the importance of wear-friction testing in the evaluation of brake pad performance. The testing is carried out in accordance with established standards, developed by taking into account the friction properties of the disc. The Brake Blown Quality Test Procedure (SAE J-661) is the standard for determining the friction properties of the brake pads in terms of friction material against the disc [48]. Moreover, when calculating the friction coefficient of the pads, the wear amount can be found by determining the weight loss. Equation (3) is used to calculate the wear rate of the friction material.

$$W(T_j) = \frac{1}{2\pi R} x \frac{A}{n} x \frac{d_1 - d_2}{f} \tag{3}$$

$W(T_j)$ = cm³/Nm at the individual j temperature
 d_1 and d_2 = the average thickness (of 5 points) of the sample
 n = the number of brake disc rotations

R = the distance between the centers of the sample and of the rotating disc
 F = the average sliding friction force
 A = the area of the sample.

F_N = Normal force
 μ = Friction coefficient

Weight loss cannot be measured accurately except by using scales that are sensitive within 103 or 104 g. If the amount of wear is expressed in grams or milligrams, then according to the friction path in meters or kilometers, the unit corresponding to the friction path is taken into consideration. If a unit is calculated for the area, it can also be found by moving from weight loss to volume loss, corresponding to the loading weight acting on the density of the material used when the amount of volume wear is to be found [49]. Equation (4) gives the formula for calculating the wear rate according to weight loss.

$$W_a = \frac{G}{dxMxs} \quad (4)$$

W_a = Wear rate (mm³/Nm)

G = Weight loss (mg)

The other method of calculating wear rate by weight loss is shown in Equation (5) [24].

$$Wear \ rate = \frac{w_0 - w_1}{s} = \frac{\Delta W}{s} = \frac{\Delta W}{2\pi r N x D x t} \quad (5)$$

w_0 = the initial weight (g)

w_1 = the final weight (g)

ΔW = the weight loss (g)

S = the sliding distance (m).

The friction coefficient (COF) is calculated by Equation (6). A schematic showing the friction and normal force applied to the brake pad according to this formula is given in Fig. 2.

$$F_s = F_N \cdot \mu \quad (6)$$

F_s = Friction force

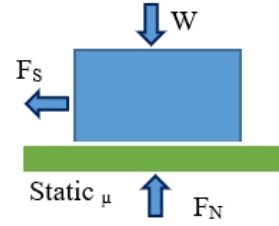


Fig. 2. Schematic view of brake pad friction

When developing brake materials and additives, a variety of tests need to be applied. These include, among others, wear, compression, hardness, thermal conductivity, and shear tests, and measurements of density. However, those that determine the brake pad friction and wear behavior are the most critical.

2.7 Laboratory-type friction devices

Once the automotive brake pads have been produced, the next, and most important step is to identify the brake pad friction and wear behavior [47]. Studies in the literature describe a number of friction testing devices, both standard and specially designed. These include inertial and friction coefficient (Chase and FAST) dynamometers, pin-on-disc testers, and tribometers, in addition to specially designed testing equipment.

2.7.1 FAST (Friction assessment and screening test) devices

The FAST devices were firstly introduced to the market by the Ford Motor Company in the mid-1960s. The brake pad samples in square block form are subjected to friction force at a certain range of temperatures by applying constant torque for 90 min [47]. Fig. 3 illustrates a schematic view of a FAST device. This device has been utilized in many studies for friction-wear testing.

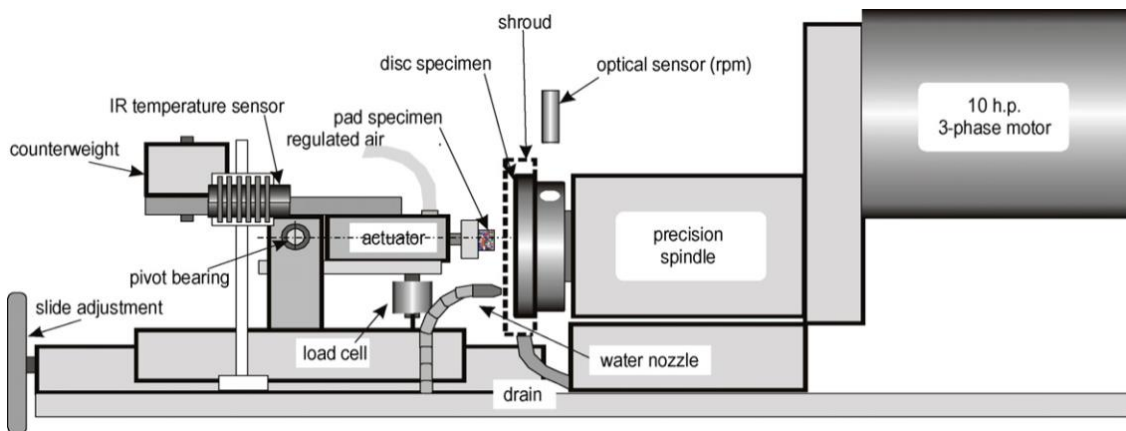


Fig. 3. Schematic view of a FAST device [33].

2.7.2 Chase-type devices

Brake dynamometers serve as excellent research devices because they enable careful control of braking parameters and testing conditions [50]. The Chase dynamometer is used to perform the test conditions of the SAE J-661 standard [48]. The Chase dynamometer includes a rotating drum with a 25.4-mm-square pad of friction material loaded against its inner diameter via an air pressure system. A small amount of friction material is rubbed against the drum to obtain data on friction and wear [50]. The losses in thickness of the drum and in weight of the pad are interpreted as the wear amount [47]. However, brake conditions

are not simulated as well as with an inertial dynamometer and thus, the Chase device is mainly used for rapid screening [2]. Fig. 4 shows a schematic view of a Chase-type device. Some researchers have utilized the Chase device to obtain wear-friction data [51]. Saffar et al. investigated the wear of rubber-based friction materials in a Chase-type device they had developed. The spinning speed was tested in the range of 200 – 700 rpm and a load of 45.4 kgf was also applied with a braking time of 10 s and 10 s release (no braking). This cycle was repeated 10 times at 150 °C [52].

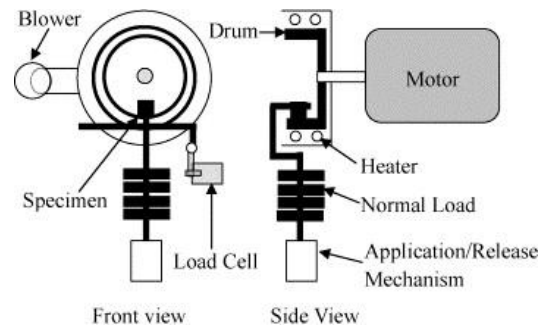


Fig. 4. Schematic view of a Chase-type device [53].

Vijay et al. [54] studied the effect of brake friction materials of pre-mixed binary metal sulphides (tin disulfide + iron disulfide) instead of antimony trisulfide on the tribological performance of the brake pad. Tribological performance tests of the brake pad were performed on the Chase friction tester according to SAE-J-661 / IS 2742 part 4. In the tests, 25 × 25 mm brake pads were rubbed against a cast iron drum (diameter 280 mm). The experimental results obtained on the Chase tester show that brake pads filled with pre-mixed binary metal sulfides have good thermal stability, physical, chemical and mechanical properties, with stable friction and less wear rate due to better lubrication that prevents friction fluctuations.

2.7.3 Krauss-type dynamometers

Krauss-type devices are only used for disc brake pads and are used to test pads attached to the carrier steel plate. In this device, pressure stages are adjusted by means of cylinders [45, 55]. Satapathy and Bijwe tested natural fiber-reinforced samples in a Krauss-type device. The authors performed braking tests at 1.82 MPa pressure according to ECE R-90 standards by applying loads of 2.5 kgf at 660 rpm at temperatures of up to 280 °C [56]. Ghazi et al. conducted experiments with a Krauss-type machine

under conditions of 660 rpm at a pressure of 1 MPa and a torque of 2.5 kgm. They were able to reach temperatures of up to 600 °C [9]. In the literature, the above parameters are usually applied, while temperature values sometimes vary [57]. Several researchers have employed the Krauss-type testing device [21, 36, 45, 57-59]. Fig. 5 presents a schematic view of a Krauss-type machine as used in these studies.

2.7.4 Full-scale inertia dynamometers

Fig. 6 illustrates a full-scale inertia dynamometer that is fully computerized for the automatic testing of four-wheeled vehicles. It has the capacity to perform brake testing in both hydraulic and air braking modes. Variable inertial loads are applied on the 175-kW motor and the torque, braking force, and COF are measured. The motor speed can be adjusted from 100 to 1550 rpm by the solid-state electronic variable speed drive with tachometer feedback. A separate box-type bed mounted on the main chassis holds the the drive motor. Gear couplings join the main shaft directly to the motor. Inertia values of 1.5 – 153.5 kg-m² can be obtained via a careful arrangement of inertia wheels (one fixed and ten attachable). A non-contact IR sensor monitors the disc/drum temperature [59].

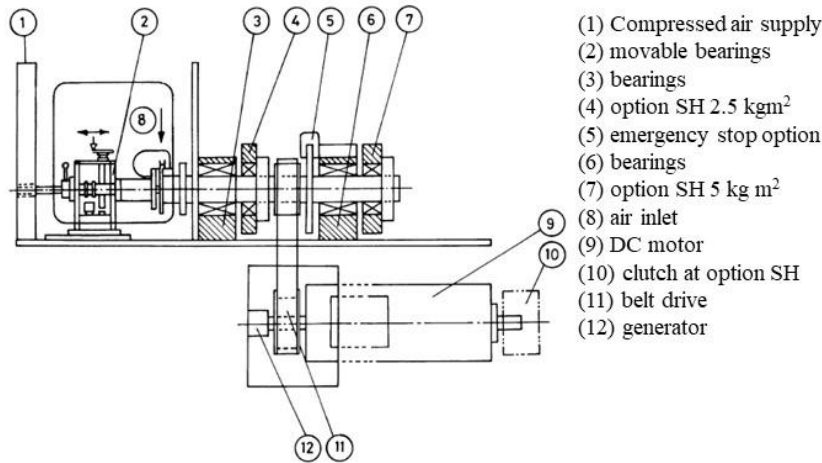
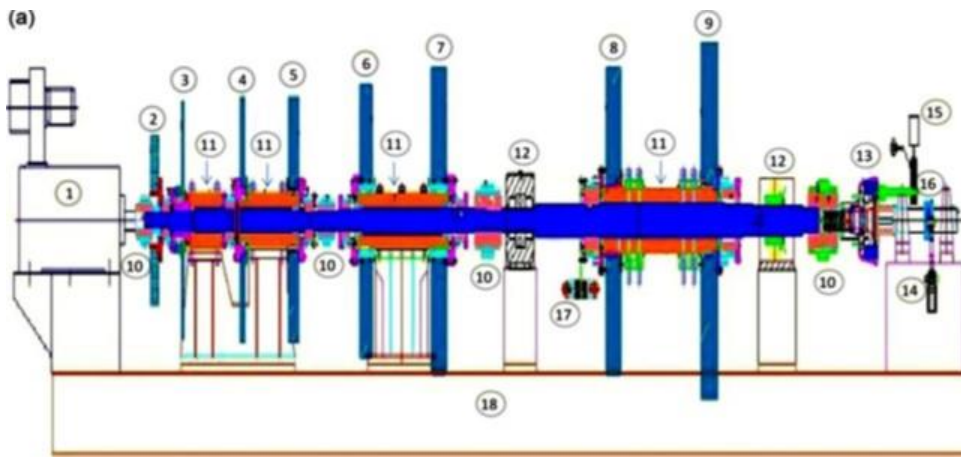


Fig. 5. Krauss-type dynamometer [57]



(1) motor, (2) flywheel of 0.5 kg-m², (3) flywheel of 2 kg-m², (4) flywheel of 4 kg-m², (5) flywheel of 8 kg-m², (6) flywheel of 16 kg-m², (7) and (8) flywheel of 32 kg-m², (9) flywheel of 64 kg-m², (10) couplings, (11) housings, (12) shaft bearings, (13) braking assembly, (14) load cell, (15) air chamber, (16) torque arm, (17) emergency brakes and (18) Dyno bed

Fig. 6. Schematic diagram of full-scale inertia dynamometer [60]

2.7.5 Pin-on-disc testers

Pin-on-disc devices can be utilized to obtain friction coefficients and wear rates in brake pad samples [61]. With the pin-on-disc apparatus, the wear-friction tests are conducted according to the ASTM: G99-05 standard [27]. The samples are prepared in accordance with the standards and mounted to the pin-on-disc for testing. The gray cast iron disc to be used in the wear-friction tests is mounted and the load is implemented according to the conditions used in the tests. Finally, the pin-on-disc tests are carried out by determining the device's turn, speed, total path distance and trajectory diameter. In the tests, the total weight loss, the COF, the variation of the COF and the sliding time are evaluated.

The weight loss for each sample can be identified via the mass method based on the TSE 555 standard and calculated by using Equation (7) [29, 62]. Fig. 7 shows a schematic view of a pin-on-disc testing device [11].

$$W = \frac{1}{2\pi R} \times \frac{1}{f m^n} \times \frac{m_1 - m_2}{\rho} \tag{7}$$

- n = the revolution of the rotating disc
- m_1 and m_2 = average weights of pre- and post-test samples (g)
- W = the specific wear rate (cm³/Nm)
- f_m = the average friction force (N)
- R = the distance between m (the center of the sample) and ρ (the density of the sample)

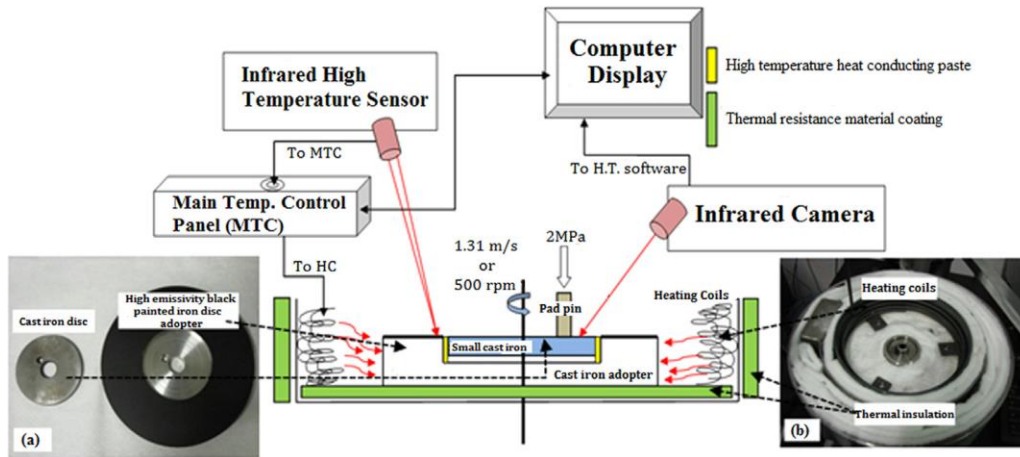
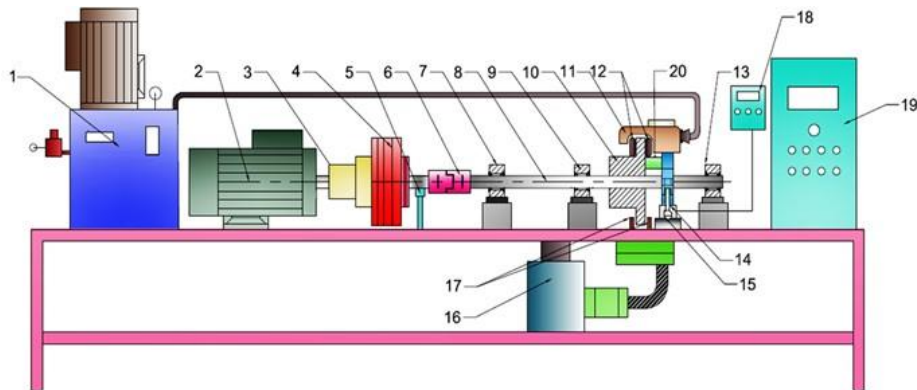


Fig. 7. Schematic view of a pin-on-disc tester

2.7.6 Specially designed friction testers

Specially designed friction testing machines have been created bearing in mind the stability and strength of the composition materials and thus, complying with all the necessary standards. Fig. 8 shows the brake pad friction-wear behavior tester developed in one study. The Fig. includes the general arrangement of the 20 components. The tester was specially designed to correspond to the real friction and wear behavior of brake pads when they come in contact with the rotor disc of an automobile. The oil fluid is directed by a hydraulic unit with proportional valves which control the opening and closing of the brake

pads on each side of the rotor disc via a piston. The main shaft supports a torque of 42.5 Nm and is rotated by an electric motor (1440 rpm, 5.5 kW) that also transmits its motion to the 240-mm gray cast iron rotor disc. The electro-magnetic clutch pad continuously transfers power at the maximum torque value of the electric motor. The electric motor and the electro-magnetic clutch are coupled to the 30-mm diameter main shaft. The bearings aid in guiding the main shaft through the the rotor disc axis. The function of the caliper is to slow down and stop the wheels [11].



(1) hydraulic unit, (2) AC motor-5.5 kW, (3) flange coupling, (4) clutch option, (5) clutch coils, (6) couplings, (7) (9) (13) bearings, (8) main shaft, (10) brake disc, (11) caliper, (12) brake pads, (14) caliper mounting apparatus, (15) load cell, (16) cooling unit, (17) heaters, (18) amplifier, (19) automation unit, and (20) infrared laser pyrometer

Fig. 8. Specially designed friction testing device [11]

2.8 Compressibility test

Compressibility is defined as the numerical constant expressing the elastic characteristics of a fluid or a solid in response to pressure on all its surfaces [63]. Compression tests are applied according to ISO 6310 and JIS D 4413 standards. The compressibility of the brake pads can be measured under two different conditions: hot and cold. According to the test standards, the pressure of 160 bars is applied during the flushing period and this process is repeated three times. Here, test loads implement a sample coupon to the force required to achieve a unit-area pressure at the contact interface. This test method can be used to assess the brake pad materials for drums of commercial vehicle discs, drum brakes or brake assemblies and material coupons for development purposes [64, 65]. When the test is finished, the amount of compression in the valve is obtained as μ and the results can be calculated in percent. The results for cold compressibility should be less than 2%, whereas those for hot compressibility should be less than 5%. Several researchers have utilized the compressibility test for brake pads. Singh et al. [58] found that the amount of compression of the cement-toothed pads they produced was between 1.07% and 1.34%. Moreover, Kachhap and Satapathy were able to achieve results in accordance with the standard, with compression rates for tungsten-augmented pads at 0.65% on average [66].

The compressive strength increases with increases in the wt. % of resin additions [27]. The plastic deformation occurring at contact points between the particles is the result of further increases in the applied pressure. The mechanical features and the quality of the particles play a significant role here [29]. The performance-composition-domain correlation of brake composites has been comprehensively demonstrated [67].

2.9 Other testing methods

Different tests have been applied to evaluate the performance of brake pads, including thermal conductivity tests, humidity ratios, surface analysis, X-ray powder diffraction (XRD) analysis, etc. In addition, a series of brake rig tests were carried out to explain how humidity influences the generation of the brake squeal and the friction coefficient [68]. Nonetheless, brake pad surface analysis is challenging because of the very coarse structure of the pads and because the soft, weak phases of their structure are easily scratched by the profilometer stylus. In addition, focus detection via optical profilometer is made almost impossible by their very low reflectivity [69]. Thermal conductivity plays a very important role in pad life. Too high thermal conductivity has a negative effect on the brake fluid, ie it creates spongy braking, while too low thermal conductivity causes higher degradation in organic components, so the thermal conductivity must be optimized for better performance. In the case of thermal stability, the higher the stability, the lower the weight loss will be, and the lower the thermal stability, the higher the weight loss due to component degradation. Optimal thermal conductivity and thermal stability are required. Thermal conductivity of brake pads can be provided by fillers. Adding volume

to the fillers in the brake pads is to reduce the cost and to add functionality to the brake pad. Scaly vermiculate is an example of functional fillings. This filler is used for heat resistance and is used to obtain a homogeneous mixture [70]. Thermal conductivity testing carried out in accordance with the ISO 7882 standard produced interesting results regarding the correlations between the thermal conductivity and the compressibility of the composites. When the conductivity and compressibility were higher, the counter-face friendliness was higher, whereas the tendency to produce hot spots was lower [71].

3. Conclusions

In this study, friction materials used for the production of brake pads and the testing devices used to determine their performance were discussed. During the course of history, brake pads have been fabricated using many different compositions. The friction materials utilized to create various brake pad compositions are the most important factors in terms of health and environmental impact, cost and performance. In addition, contribution to the local economy is taken into consideration with brake pads produced using local materials. The advance of technology and the depletion of some natural resources have also made it clear that there is a need for future research into the use of alternative components in the production of brake pads. Performance testing of newly created compositions is important for the commercialization of these novel brake pads. Consequently, opportunities have been presented for the utilization of the high-performance testing devices introduced in this study, the results of which can be summarized as follows:

- The composition of the brake pad to be produced is one of the most important factors affecting performance. The testing phase is crucial when formulating new brake pads
- Friction-wear tests of brake pads are carried out using FAST-type devices, Chase-type devices, Krauss-type dynamometers, full-scale inertia dynamometers, pin-on-disc testers and specially designed friction testers.
- Other tests for evaluation of brake pad performance include those for measuring hardness, density, porosity, and water and oil absorption as well as shear tests, SEM and EDAX microstructure analyses, compressibility tests, XRD analyses, surface analyses, thermal conductivity tests and so forth.

Conflict of Interest Statement

The authors declare that there is no conflict of interest.

CRedit Author Statement

Gülşah Akıncioğlu: Conceptualization, Writing-original draft, **Sıtkı Akıncioğlu:** Visualization, Writing-original draft, **Hasan Öktem:** Supervision, **İlyas Uygur:** Project administration, Validation.

References

- [1] Ibhadode A. O. A., M. DI. Development of Asbestos-Free Friction Lining Material from Palm Kernel Shell. *J of the Braz Soc of Mech Sci & Eng.* 2008;2(2):166-73.
- [2] Tsang PHS, Jacko MG, Rhee SK. Comparison of Chase and inertial brake Dynamometer testing of automotive friction materials. *Wear.* 1985;103(3):217-32.
- [3] Eriksson M. Friction and contact phenomena of disc brakes related to squeal: Citeseer; 2000.
- [4] Mikael Erikssona JL, Staffan Jacobson. Wear and contact conditions of brake pads: dynamical in situ studies of pad on glass. *Wear.* 2001;249:272-8.
- [5] Almaslow A, Ghazali MJ, Talib RJ, Ratnam CT, Azhari CH. Effects of epoxidized natural rubber–alumina nanoparticles (ENRAN) composites in semi-metallic brake friction materials. *Wear.* 2013;302(1–2):1392-6.
- [6] Vijay R, Manoharan S, Arjun S, Vinod A, Singaravelu DLJJoNF. Characterization of silane-treated and untreated natural fibers from stem of leucas aspera. 2020:1-17.
- [7] Manoharan S, Shihab AI, Alemdar ASA, Babu LG, Vijay R, Singaravelu DLJMRE. Influence of recycled basalt-aramid fibres integration on the mechanical and thermal properties of brake friction composites. 2019;6(11):115310.
- [8] H. Jang, J.S. Lee, Fash JW. Compositional effects of the brake friction material on creep groan phenomena. *Wear.* 2001;251:1477-83.
- [9] A.A.S. Ghazi, K. Chandra, Misra PS. Development and Characterization of Fe-Based Friction Material Made by Hot Powder Preform Forging for Low Duty Applications. *Journal of Minerals & Materials Characterization & Engineering.* 2011;10(13):1205-12.
- [10] Satapathy BK. Fade and Recovery Behavior of Non-Asbestos Organic (NAO) Composite Friction Materials based on Combinations of Rock Fibers and Organic Fibers. *Journal of Reinforced Plastics and Composites.* 2005;24(6):563-77.
- [11] Kim SS, Hwang HJ, Shin MW, Jang H. Friction and vibration of automotive brake pads containing different abrasive particles. *Wear.* 2011;271(7-8):1194-202.
- [12] Kumar M, Bijwe J. Non-asbestos organic (NAO) friction composites: Role of copper; its shape and amount. *Wear.* 2011;270(3-4):269-80.
- [13] W.B.WanNik AFA, S. Syahrullail, H.H. Masjuki, M.F. Ahmad. The Effect Of Boron Friction Modifier On The Performance Of Brake Pads. *International Journal of Mechanical and Materials Engineering (IJMME).* 2012;7(1):31-5.
- [14] Qi S, Fu Z, Yun R, Jiang S, Zheng X, Lu Y, et al. Effects of walnut shells on friction and wear performance of eco-friendly brake friction composites. *Proceedings of the Institution of Mechanical Engineers, Part J: Journal of Engineering Tribology.* 2014;228(5):511-20.
- [15] Singaravelu DL, Vijay R, Manoharan S, Kchaou MJJoA, Engineering M. Development and performance evaluation of eco-friendly crab shell powder based brake pads for automotive applications. 2019;16(2):6502-23.
- [16] Manoharan S, Krishnan GS, Babu LG, Vijay R, Singaravelu DLJMRE. Synergistic effect of red mud-iron sulfide particles on fade-recovery characteristics of non-asbestos organic brake friction composites. 2019;6(10):105311.
- [17] Nagesh SN, Siddaraju C, Prakash SV, Ramesh MR. Characterization of Brake Pads by Variation in Composition of Friction Materials. *Procedia Materials Science.* 2014;5:295-302.
- [18] Bahari SA, Isa KH, Kassim MA, Mohamed Z, Othman EA. Investigation on hardness and impact resistance of automotive brake pad composed with rice husk dust. 2012:155-61.
- [19] Fan S, Zhang L, Cheng L, Zhang J, Yang S, Liu H. Wear mechanisms of the C/SiC brake materials. *Tribology International.* 2011;44(1):25-8.
- [20] Kukutschová J, Roubíček V, Mašláň M, Jančík D, Slovák V, Malachová K, et al. Wear performance and wear debris of semimetallic automotive brake materials. *Wear.* 2010;268(1-2):86-93.
- [21] Stadler Z, Krnel K, Kosmac T. Friction behavior of sintered metallic brake pads on a C/C–SiC composite brake disc. *Journal of the European Ceramic Society.* 2007;27(2-3):1411-7.
- [22] Rajan BS, Balaji MS, Saravanakumar SJMRE. Effect of chemical treatment and fiber loading on physico-mechanical properties of Prosopis juliflora fiber reinforced hybrid friction composite. 2018;6(3):035302.
- [23] Rajan BS, Balaji M, Noorani AMA, Khateeb MUH, Hariharasakthisudan P, Doss PAJMRE. Tribological performance evaluation of newly synthesized silane treated shell powders in friction composites. 2019;6(6):065317.
- [24] Ademoh NA, Olabisi AI. Development and evaluation of maize husks (asbestos-free) based brake pad. *Development.* 2015;5(2).
- [25] Maleque M, Atiqah A, Talib R, Zahurin H. New natural fibre reinforced aluminium composite for automotive brake pad. *International Journal of Mechanical and Materials Engineering.* 2012;7(2):166-70.
- [26] V. S. Aigbodion, U. Akadike, S.B. Hassan, F. Asuke, Agunsoye JO. Development of Asbestos -Free Brake Pad Using Bagasse. *Tribology in industry.* 2010;32(1):12-8.
- [27] Idris U, Aigbodion V, Abubakar I, Nwoye C. Eco-friendly asbestos free brake-pad: using banana peels. *Journal of King Saud University-Engineering Sciences.* 2015;27(2):185-92.
- [28] Manoharan S, Vijay R, Singaravelu DL, Kchaou MJAJfS, Engineering. Experimental investigation on the tribo-thermal properties of brake friction materials containing various forms of graphite: a comparative study. 2019;44(2):1459-73.
- [29] Ertan R, Yavuz N. An experimental study on the effects of manufacturing parameters on the tribological properties of brake lining materials. *Wear.* 2010;268(11-12):1524-32.
- [30] Mutlu I, Oner C, Findik F. Boric acid effect in phenolic composites on tribological properties in brake linings. *Materials & Design.* 2007;28(2):480-7.
- [31] Saffar A, Shojaei A. Effect of rubber component on the performance of brake friction materials. *Wear.* 2012;274-275:286-97.

- [32] Öktem H, Uygur İ, Akincioglu G, Kır D, Karakaş H. Evaluation of non-asbestos high performance brake pads produced with organic dusts.
- [33] Blau PJ, McLaughlin JC. Effects of water films and sliding speed on the frictional behavior of truck disc brake materials. *Tribology International*. 2003;36(10):709-15.
- [34] Saikrishnan G, Jayakumari L, Vijay RJIL, Tribology. Influence of iron–aluminum alloy on the tribological performance of non-asbestos brake friction materials—a solution for copper replacement. 2019.
- [35] Ma Y, Martynková GS, Valášková M, Matějka V, Lu Y. Effects of ZrSiO₄ in non-metallic brake friction materials on friction performance. *Tribology International*. 2008;41(3):166-74.
- [36] Singh T, Patnaik A. Performance assessment of lapinus–aramid based brake pad hybrid phenolic composites in friction braking. *Archives of Civil and Mechanical Engineering*. 2015;15(1):151-61.
- [37] Yun R, Filip P, Lu Y. Performance and evaluation of eco-friendly brake friction materials. *Tribology International*. 2010;43(11):2010-9.
- [38] Mohanty S, Chugh YP. Development of fly ash-based automotive brake lining. *Tribology International*. 2007;40(7):1217-24.
- [39] Xin X, Xu CG, Qing LF. Friction properties of sisal fibre reinforced resin brake composites. *Wear*. 2007;262(5-6):736-41.
- [40] Fu Z, Suo B, Yun R, Lu Y, Wang H, Qi S, et al. Development of eco-friendly brake friction composites containing flax fibers. *Journal of Reinforced Plastics and Composites*. 2012;31(10):681-9.
- [41] Fan Y, Matějka V, Kratošová G, Lu Y. Role of Al₂O₃ in Semi-Metallic Friction Materials and its Effects on Friction and Wear Performance. *Tribology Transactions*. 2008;51(6):771-8.
- [42] Vijay R, Lenin Singaravelu D, Filip P. Influence of molybdenum disulfide particle size on friction and wear characteristics of non-asbestos-based copper-free brake friction composites. *Surface Review and Letters*. 2020;27(01):1950085.
- [43] Singaravelu DL, Vijay R, Filip P. Influence of various cashew friction dusts on the fade and recovery characteristics of non-asbestos copper free brake friction composites. *Wear*. 2019;426:1129-41.
- [44] Mikael Eriksson SJ. Tribological surfaces of organic brake pads. *Tribology International*. 2000;33:817-27.
- [45] Dadkar N, Tomar BS, Satapathy BK. Evaluation of flyash-filled and aramid fibre reinforced hybrid polymer matrix composites (PMC) for friction braking applications. *Materials & Design*. 2009;30(10):4369-76.
- [46] Han Y, Tian X, Yin Y. Effects of Ceramic Fiber on the Friction Performance of Automotive Brake Lining Materials. *Tribology Transactions*. 2008;51(6):779-83.
- [47] Blau PJ. Compositions, functions, and testing of friction brake materials and their additives. Oak Ridge National Lab., TN (US); 2001.
- [48] SAE S. J2396 Surface Vehicle Recommended Practice, Definitions and Experimental Measures Related to the Specification of Driver Visual Behavior Using Video Based Techniques. Society of Automotive Engineers, Warrendale, Pa, USA; 2000.
- [49] Bijwe J. Composites as friction materials: Recent developments in non-asbestos fiber reinforced friction materials—a review. *Polymer composites*. 1997;18(3):378-96.
- [50] Alnaqi AA, Barton DC, Brooks PC. Reduced scale thermal characterization of automotive disc brake. *Applied Thermal Engineering*. 2015;75:658-68.
- [51] Qu J, Blau PJ, Jolly BC. Oxygen-diffused titanium as a candidate brake rotor material. *Wear*. 2009;267(5–8):818-22.
- [52] Saffar A, Shojaei A, Arjmand M. Theoretical and experimental analysis of the thermal, fade and wear characteristics of rubber-based composite friction materials. *Wear*. 2010;269(1-2):145-51.
- [53] Zhang S, Wang F. Comparison of friction and wear performances of brake materials containing different amounts of ZrSiO₄ dry sliding against SiCp reinforced Al matrix composites. *Materials Science and Engineering: A*. 2007;443(1–2):242-7.
- [54] Vijay R, Manoharan S, Nagarajan SJIL, Tribology. Influence of premixed dual metal sulfides on the tribological performance of copper-free brake friction materials. 2020.
- [55] Singh T, Patnaik A, Chauhan R, Rishiraj A. Assessment of braking performance of lapinus–wollastonite fibre reinforced friction composite materials. *Journal of King Saud University - Engineering Sciences*. 2015.
- [56] Satapathy BK, Bijwe J. Performance of friction materials based on variation in nature of organic fibres. *Wear*. 2004;257(5-6):573-84.
- [57] Gurunath PV, Bijwe J. Friction and wear studies on brake-pad materials based on newly developed resin. *Wear*. 2007;263(7-12):1212-9.
- [58] Singh T, Patnaik A, Chauhan R. Optimization of tribological properties of cement kiln dust-filled brake pad using grey relation analysis. *Materials & Design*. 2016;89:1335-42.
- [59] Patnaik A, Kumar M, Satapathy BK, Tomar BS. Performance sensitivity of hybrid phenolic composites in friction braking: Effect of ceramic and aramid fibre combination. *Wear*. 2010;269(11–12):891-9.
- [60] Chiranjit Sarkar, Hirani H. Frictional Characteristics of Brake Pads using Inertia Brake Dynamometer. *International Journal of Current Engineering and Technology*. 2015;5(2):981-9.
- [61] Yi G, Yan F. Effect of hexagonal boron nitride and calcined petroleum coke on friction and wear behavior of phenolic resin-based friction composites. *Materials Science and Engineering: A*. 2006;425(1-2):330-8.
- [62] Verma PC, Ciudin R, Bonfanti A, Aswath P, Straffellini G, Gialanella S. Role of the friction layer in the high-temperature pin-on-disc study of a brake material. *Wear*. 2016;346:56-65.
- [63] Steege R, Marx F. A new approach to material compressibility of brake pads. SAE Technical Paper; 2008. Report No.: 0148-7191.
- [64] Sasaki Y, Tanaka T. Harmonization Activities on ISO and JIS Standards (Compressibility-2) for Brake Linings in Japan. SAE International; 2003.

- [65] Sasaki Y, Kaido M. Harmonization Activities on ISO and JIS Standards (Assembly Shear Strength) for Brake Linings in Japan. SAE International; 2002.
- [66] Kachhap RK, Satapathy BK. Synergistic effect of tungsten disulfide and cenosphere combination on braking performance of composite friction materials. *Materials & Design*. 2014;56:368-78.
- [67] Kumar M, Satapathy BK, Patnaik A, Kolluri DK, Tomar BS. Evaluation of fade-recovery performance of hybrid friction composites based on ternary combination of ceramic-fibers, ceramic-whiskers, and aramid-fibers. *Journal of Applied Polymer Science*. 2012;124(5):3650-61.
- [68] Eriksson M, Lundqvist A, Jacobson S. A study of the influence of humidity on the friction and squeal generation of automotive brake pads. *Proceedings of the Institution of Mechanical Engineers, Part D: Journal of Automobile Engineering*. 2001;215(3):329-42.
- [69] Eriksson M, Bergman F, Jacobson S. Surface characterisation of brake pads after running under silent and squealing conditions. *Wear*. 1999;232(2):163-7.
- [70] Thiyagarajan V, Kalaichelvan K, Vijay R, Singaravelu DLJJotBSOMS, Engineering. Influence of thermal conductivity and thermal stability on the fade and recovery characteristics of non-asbestos semi-metallic disc brake pad. 2016;38(4):1207-19.
- [71] Kumar M, Boidin X, Desplanques Y, Bijwe J. Influence of various metallic fillers in friction materials on hot-spot appearance during stop braking. *Wear*. 2011;270(5-6):371-81.